Available online at www.sciencedirect.com
SCIENCE DIRECT®
European Polymer Journal 41 (2005) 1115–1122
EUROPEAN POLYMER JOURNAL
www.elsevier.com/locate/europolj

Preparation and properties of compatibilized LDPE/organo-modified montmorillonite nanocomposites

J. Morawiec [a], A. Pawlak [a], M. Slouf [b], A. Galeski [a,*], E. Piorkowska [a], N. Krasnikowa [a,1]

[a] Centre of Molecular and Macromolecular Studies, Polish Academy of Sciences, Sienkiewicza 112, 90-363 Lodz, Poland
[b] Institute of Macromolecular Chemistry, Czech Academy of Sciences, Heyrovskeho nam. 2, 16206 Prague, Czech Republic

Received 23 June 2004; received in revised form 5 November 2004; accepted 12 November 2004
Available online 5 January 2005

Abstract

Nanocomposites based on low density polyethylene, containing of 3 or 6 wt.% of organo-modified montmorillonite nanoclay (MMT-ODA) and maleic anhydride grafted low density polyethylene as a compatibilizer were prepared by melt mixing and characterized. Exfoliation of silicate layers was achieved, as confirmed by X-ray diffraction and transmission electron microscopy. The compatibilized nanocomposites exhibit improved thermal stability in air as compared to neat polyethylene and nonexfoliated MMT-ODA composite. The crystallinity and crystallization kinetics of polyethylene matrix is not affected significantly by the presence of MMT-ODA clay. Drawability of the compatibilized nanocomposite with 6 wt.% of MMT-ODA is similar to neat polyethylene, whereas the composition having the same amount of MMT-ODA, without compatibilizer, exhibits poorer drawability. Scanning electron microscopy and density measurements of drawn samples indicate the existence of pores in noncompatibilized composite while no pores and good adhesion to MMT-ODA are found in compatibilized nanocomposites.

Keywords: Low density polyethylene based nanocomposites; Montmorillonite; Tensile properties; Crystallization

1. Introduction

Polymer-layered silicate nanocomposites are a new class of materials with improved barrier properties, reduced flammability (e.g. [1–4]) and mechanical properties modified as compared to those of neat polymers (e.g. [4–6]). Methods of exfoliation of silicate layers are well developed for application to many polymers. Frequently, organic modification of a clay is necessary to increase the compatibility with a polymer and to enlarge the interlayer distance. The routes to obtain isotactic polypropylene (iPP) based nanocomposites with organo-modified montmorillonite (o-MMT) and the description of material properties, recently reviewed in Ref. [7], include application of anhydrides—modified propylene oligomers as compatibilizers for iPP/clay systems [8,9]. Polyethylene (PE) based nanocomposites with o-MMT were also obtained [10–19] by different methods including polymerization of PE in the presence of layered silicate [10–12] and application of polyethylene-grafted-maleic anhydride (PE-g-MA) as a matrix

* Corresponding author. Tel.: +48 42 681 5761; fax: +48 42 684 7126.
E-mail address: andgal@bilbo.cbmm.lodz.pl (A. Galeski).
[1] Permanent address: Topchiev Institute of Petrochemical Synthesis, Russian Academy of Sciences, Leninsky Prospekt 29, 117912 Moscov, Russia.

0014-3057/$ - see front matter © 2004 Elsevier Ltd. All rights reserved.
doi:10.1016/j.eurpolymj.2004.11.011

[13,14]. In Ref. [13] the exfoliation in PE-g-MA systems with filler content up to 5 wt.% was achieved. Elevation of Young modulus, marginal increase of the yield stress, elevation of crystallization temperature and crystallinity decrease were reported for exfoliated nanocomposite.

Wang et al. [15] used two grades, commercial and laboratory synthesized linear low density PE (LLDPE), PE-g-MA, laboratory synthesized LLDPE-g-MA and LLDPE reacted with PE-g-MA for preparation of silicate nanocomposites by melt mixing. The clay exfoliation was achieved in LLDPE based system when the clay was properly chemically modified and maleic anhydride group content in compatibilizers was larger than 0.1 wt.%. Some increase of crystallization and melting temperatures together with the decrease of crystallinity were found in those nanocomposites [16].

Recently, an application of LLDPE-g-MA as a compatibilizer for HDPE/o-MMT system [17] led to the improved barrier properties accompanied by significant increase of the elastic modulus as compared with HDPE/LLDPE-g-MA blends.

Low density polyethylene (LDPE), a widely used packaging material, seems to be specially attractive for nanocomposite preparation, mostly due to the expected improvement of barrier properties. However, the information about such nanocomposites, with PE-g-MA, as a compatibilizer, is scarce [18]. The effectiveness of nanoclay exfoliation in LDPE based nanocomposite in Ref. [18] was much worse than in HDPE based system because of more difficult penetration of branched LDPE macromolecules into clay galleries. The properties of LDPE based compositions were not characterized.

In our studies we have prepared exfoliated LDPE based nanocomposites with organo-modified clay and anhydride grafted low density polyethylene according to the protocol elaborated by us earlier for iPP based nanocomposites [19]. The properties of obtained systems were also characterized.

2. Experimental

LDPE Lupolen 1840D with $M_w = 4.5 \times 10^5$ g/mol, MFI = 0.3 g/10 min (190 °C, 2.16 kg), and density 0.919 g/cm^3, was supplied by BASF AG. Montmorillonite clay (MMT-ODA) was octadecyl amine modified Nanomer I30P from Nanocor (USA) with the interlayer distance of 2.2 nm, having particle size within a range 16–20 μm and density 1.9 g/cm^3. Ultra low density PE-g-MA polyethylene, Primaflex AF64W, produced by Enichem, $M_w = 1.29 \times 10^5$ g/mol, MFI = 1.6 g/10 min (190 °C, 2.16 kg) with 0.5–1% of maleic anhydride groups and density of 0.885 g/cm^3, was selected as a compatibilizer.

The compositions of LDPE/PE-g-MA/MMT-ODA were prepared in the Brabender internal mixer in two steps mixing procedure. First, PE-g-MA/MMT-ODA masterbatch was prepared by mixing PE-g-MA with the clay in weight proportion of 2:1, at 160 °C, for 20 min, at the speed of 60 rpm. In the second step, the masterbatch was blended with LDPE at 190 °C for 20 min, at 60 rpm. Two compositions of LDPE/PE-g-MA/MMT-ODA were prepared, having the weight proportions of 91:6:3 and 82:12:6. A composite of 94 wt.% LDPE with 6 wt.% of MMT-ODA and also a blend of LDPE with 13 wt.% of PE-g-MA were also obtained for comparison in one step blending at 190 °C, for 20 min, at 60 rpm. Neat LDPE was also processed in the same way.

For further studies 1 mm thick films of all materials were compression moulded between stainless steel plates at 190 °C for 2 min, followed by quenching in water bath at room temperature. Oar shaped samples with gauge length of 9.5 mm, according to ASTM D638, and samples for differential scanning calorimetry (DSC) and for thermogravimetry (TGA) having a mass of 8–10 mg and 25–30 mg, respectively, were cut out from the films.

The effectiveness of MMT-ODA exfoliation and the crystal structure of PE were studied using wide angle X-ray diffraction (WAXS) in transmission (2Θ range from 1° to 9°) and in reflection mode (2Θ range from 10° to 45°), respectively. Computer controlled wide angle goniometer coupled to a sealed-tube source of Cu K_α radiation, operating at 30 kV and 30 mA, was used. The Cu K_α line was filtered using electronic filtering and the usual thin Ni filter. 2Θ scans were collected with a divergence angle of less than 0.05°. Long period of PE was probed by 2-D small angle X-ray scattering (2-D SAXS). The 1.1 m long Kiessig-type vacuum camera, coupled to the X-ray generator (sealed-tube, fine point Cu K_α Ni filtered source operating at 50 kV and 35 mA, Philips), was equipped with a capillary collimator (X-Ray Optical Systems Inc.) allowing for the resolution of scattering objects up to 40 nm. The Kodak imaging plates, used as a recording medium, after exposition were analyzed with PhosphorImager SI system (Molecular Dynamics).

For further studies of exfoliation degree a transmission electron microscope (TEM) JEM 200 CX (Jeol, Japan) operating at 100 kV, equipped with digitizing camera DXM1200 (Nikon) was used. The ultrathin sections for TEM were cut by ultramicrotome Leica Ultracut UCT (equipped with cryoattachment) at −110 °C.

Thermal properties of materials were determined by DSC, TA Instruments 2920. Samples were heated from −10 to 160 °C, melt annealed for 3 min, cooled down and heated again at the rate of 10 K/min. Melting of PE-g-MA was also studied in the temperature range from −30 to 160 °C. Thermal stability was determined by TA Instruments TGA 2950 thermogravimetric analyzer during heating at the rate of 20 K/min from 20 to 600 °C, in air and in dry N_2.

Tensile tests were performed on Instron Tensile Testing Machine model 5582 at room temperature and at the deformation rate of 50%/min using at least 5 specimens of each material. Morphology of sample surfaces after tensile test was examined by Jeol 5500LV scanning electron microscope (SEM). Density of materials, prior and after the deformation to elongation ratio about 4, was measured by a floatation method in a mixture of water and ethanol.

3. Results

During mixing of PE-g-MA with MMT-ODA the increase of melt temperature to 200 °C with mixing time was observed. The torque during mixing, 32 N m, was twice as that measured for neat LDPE processed at the same conditions. During mixing of the masterbatch with LDPE the temperature increased to 200–210 °C, but torque level was constant at about 16 N m.

X-ray diffractograms of materials studied are presented in Fig. 1A and B. A wide peak for LDPE/MMT-ODA 94:6 wt.% sample resulted from layered MMT-ODA structure.. In both compatibilized compositions the peak significantly decreased, indicating good exfoliation of MMT-ODA clay in the PE matrix, although the exfoliation was less complete in LDPE/PE-g-MA/MMT-ODA 82:12:6 wt.% than in LDPE/PE-g-MA/MMT-ODA 81:6:3 wt.%. In all materials pronounced peaks from crystallographic planes (1 1 0) and (2 0 0) of PE orthorhombic form are clearly visible, in Fig. 1B where the exemplary X-ray diffractograms are plotted for the respective range of 2θ angles. There are no noticeable differences between the materials studied.

TEM micrographs show partial exfoliation in the masterbatch (PE-g-MA/MMT-ODA 67:33 wt.%), and in both compatibilized nanocomposites (Fig. 2). The exfoliation seemed to be more pronounced in the compatibilized nanocomposite with 3 wt.% of the clay than in the system with 6 wt.% of the clay, which conforms to the X-ray diffraction results (Fig. 1A). The sample without compatibilizer exhibited no exfoliation in TEM micrographs (Fig. 2), which agreed with the diffraction results as well (Fig. 1A).

The striking difference between the structure of composition of LDPE with the clay and the masterbatch of PE-g-MA/MMT-ODA demonstrates clearly the influence of grafted groups of the compatibilizer on the interactions between the filler and the polymer, allowing PE-g-MA chains to access between platelets of the clay.

The DSC studies of melting–crystallization–melting cycles have not shown any significant differences between the thermal behaviour of samples as it is visible in Fig. 3, where the exemplary thermograms are plotted. The crystallization temperature, crystallinity level and the melting temperatures during the first heating are collected in Table 1. In each case, during the first heating the melting started early, below room temperature, and achieved a peak rate at about 107–108.5 °C. On the ascending slope of the main peak the shoulder was recognizable, at about 46.5–49 °C. Also the crystallization of all materials proceeded in a similar way; with the main peak around 94.5–94 °C and the small peak around 56.5–59 °C. There was no difference in crystallization temperatures neither between LDPE/PE-g-MA/MMT-ODA 82:12:6 wt.% and the LDPE/PE-g-MA blend nor between a neat LDPE and LDPE/MMT 94:6 wt.%. This behaviour indicates no significant nucleation activity of MMT-ODA in the LDPE based systems and it is different than that found in HDPE based [13,16] and iPP based [20–22] compositions with nanoclay, where pronounced elevation of crystallization temperature due to nucleation activity of the clay was observed. The second heating

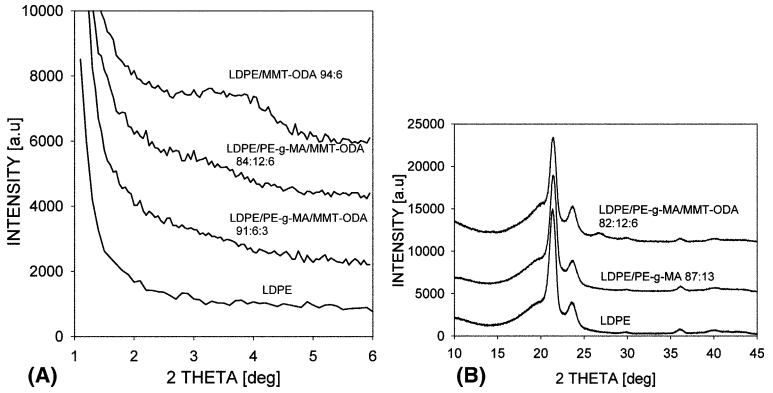

Fig. 1. (A) X-ray diffractograms in the range of 2θ angles from 1° to 6° for LDPE/MMT-ODA 94:6 wt.%, LDPE/PE-g-MA/MMT-ODA 82:12:6 wt.%, LDPE/PE-g-MA/MMT-ODA 91:6:3 wt.% and LDPE. (B) X-ray diffractograms in the range of 2θ angles from 10° to 45° for LDPE, LDPE/PE-g-MA 87:13 wt.% and LDPE/PE-g-MA/MMT-ODA 82:12:6 wt.%.

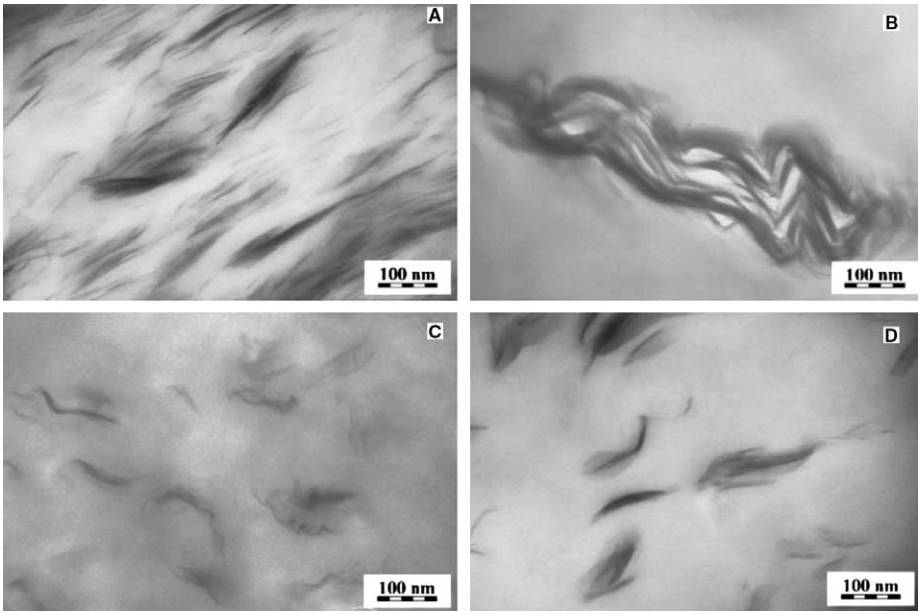

Fig. 2. TEM micrographs of ultrathin sections of PE-g-MA/MMT-ODA masterbatch (A), LDPE/MMT-ODA 94:6 wt.% (B), LDPE/PE-g-MA/MMT-ODA 91:6:3 wt.% (C) and LDPE/PE-g-MA/MMT-ODA 82:12:6 wt.% (D).

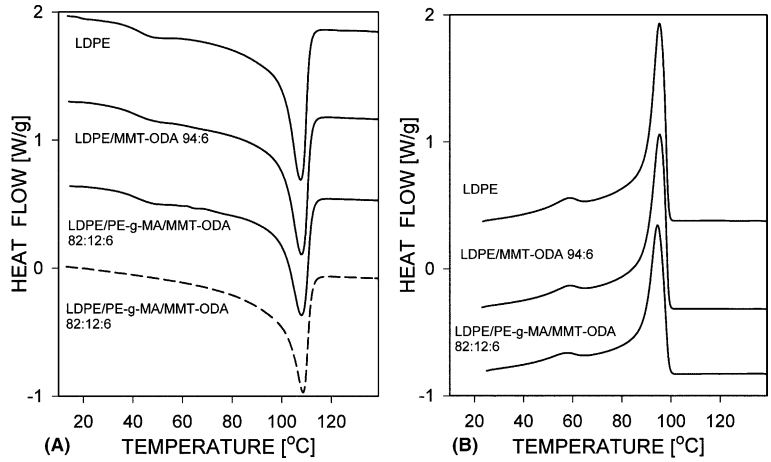

Fig. 3. DSC thermograms of LDPE, LDPE/MMT-ODA 94:6 wt.% and LDPE/PE-g-MA/MMT-ODA 82:12:6 wt.%: (A) heating: solid line—first heating, dashed line—second heating; (B) cooling.

was similar to the first heating, except that the shoulder did not appear on the ascending slope of the main peak, thus, it was probably associated with melting of a fraction of small crystals formed during quenching of the samples. The crystallinity of polymer matrix, assuming the heat of fusion of 293 J/g [23], recalculated to the content of both polymeric components, was the highest (44%) for materials without PE-g-MA, the lowest (39%) for the nanocomposite with 6 wt.% of MMT-ODA and LDPE/PE-g-MA blend and intermediate (41%) for LDPE/PE-g-MA/MMT-ODA 91:6:3 wt.%. Thus, the differences should be attributed to the presence of PE-g-MA rather than to the filler, especially that the enthalpy of melting of PE-g-MA is about half of that of neat LDPE.

The long period as determined by the SAXS method, listed in Table 1, is in the range of 11.6–11.9 for all samples. These results indicate that neither MMT-ODA nor PE-g-MA influenced the lamellar crystallization of the systems studied in a significant way.

Table 1
Crystallization temperatures, crystallinity levels and melting temperatures determined by DSC method during the first heating and the long period of materials determined by SAXS

Material code	Crystallization temperature [°C]	Melting temperature [°C]	Crystallinity [%]	Long period [nm]
LDPE	95.3	107.6	44	11.6
LDPE/MMT-ODA 94:6	95.3	107.9	44	11.6
LDPE/PE-g-MA/MMT-ODA 91:6:3	94.8	108.5	41	11.7
LDPE/PE-g-MA/MMT-ODA 82:12:6	94.5	108.0	39	11.9
LDPE/PE-g-MA 87:13	94.6	107.1	39	11.8

Crystallinity levels calculated per polymer content assuming heat of fusion of 293 J/g.

The thermogravimetric curves recorded in N_2 atmosphere, plotted in Fig. 4, show the decomposition of all materials starting slowly at about 370 °C. The process in neat LDPE and in the blend of LDPE with 13% of PE-g-MA was similar, with peak intensity at 485 °C, leaving above 510 °C a residue of 0.15 wt.%. The decompositions of all materials containing MMT-ODA was initially slower but reached peak intensity and ended at lower temperatures (500–510 °C) than in samples without MMT-ODA. The level of residue was 4.0 and 2 wt.%. for compositions with 6 wt.% of MMT-ODA and for the nanocomposite with 3 wt.% of MMT-ODA, respectively. Thus, the filler presence did not improve the thermal stability of the material, independently whether it underwent the exfoliation or not.

Differences between the materials have shown up during heating in air, as it is demonstrated in Fig. 5. The weight loss in air started at around 250 °C for LDPE, LDPE/PE-g-MA blend and LDPE/MMT-ODA composite, while at 300 °C for both compatibilized nanocomposites. Weight loss intensity of LDPE

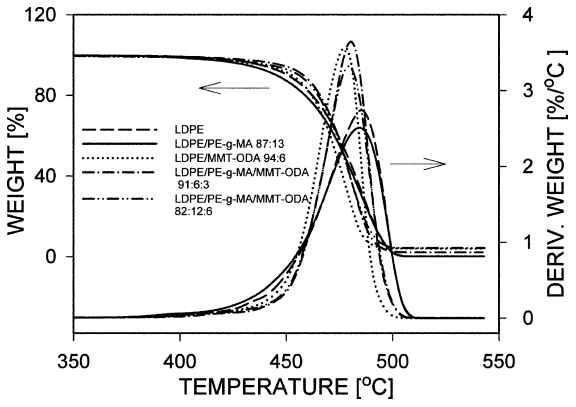

Fig. 4. Temperature dependence of weight loss and its first derivative with respect to temperature during heating in N_2 for LDPE, LDPE/PE-g-MA 87:13 wt.%, LDPE/MMT-ODA 94:6 wt.%, LDPE/PE-g-MA/MMT-ODA 91:6:3 wt.% and LDPE/PE-g-MA/MMT-ODA 82:12:6 wt.%.

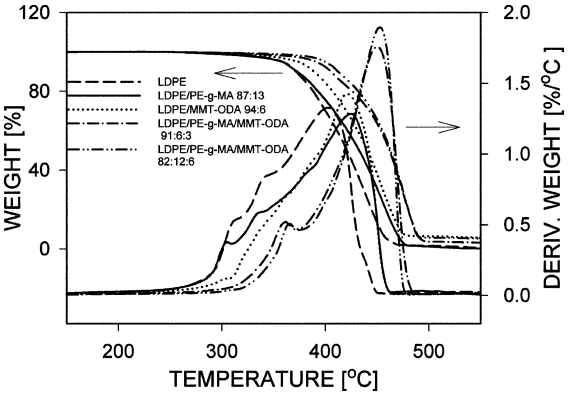

Fig. 5. Temperature dependence of weight loss and its first derivative with respect to temperature during heating in air for LDPE, LDPE/PE-g-MA 87:13 wt.%, LDPE/MMT-ODA 94:6 wt.%, LDPE/PE-g-MA/MMT-ODA A91:6:3 wt.% and LDPE/PE-g-MA/MMT-ODA 82:12:6 wt.%.

achieved a main peak at 440 °C and lasted until 470 °C leaving a small residue of 2 wt.% which decreased finally to 0.2% at 600 °C. The decomposition of the blend of LDPE with compatibilizer was similar to that of neat LDPE, except that the peak intensity and the end were reached at the temperatures higher by approximately 15 °C than those for neat LDPE. The weight loss of the composite LDPE/MMT-ODA 94:6 wt.% achieved the maximum rate at 454 °C and ended at 480 °C. During heating above that temperature only a small decrease of residues from 6.6% to 4.7% was detected. In both nanocomposites, with 3 and 6 wt.% of MMT-ODA, the decomposition achieved a maximum rate at 475–477 °C and ended at about 495–500 °C. At higher temperature only the slow decrease of residues of 3.7% and 5.7% to 1.3% and 1.6%, respectively, was registered. On the ascending slopes of the main peaks of the weight loss rate the pronounced shoulders were visible for neat LDPE and its blend with the compatibilizer, while for the compatibilized nanocomposites prior to the main peaks, the additional peaks around 409–411 °C were observed. The increase of peak temperature

Table 2
Tensile properties and the density before and after deformation of the materials

Composition [wt.%]	Young modulus [MPa]	Yield stress [MPa]	Stress at break [MPa]	Elongation at break [%]	Initial density [g/cm^3]	Density after deformation [g/cm^3]
LDPE	98.7	9.1	13.6	652	0.918	0.921
LDPE/MMT-ODA 94:6	108.4	9.5	10.9	363	0.944	0.902
LDPE/PE-g-MA 87:13	92.0	8.0	14.3	821	–	–
LDPE/PE-g-MA/MMT-ODA 91:6:3	100.8	9.0	10.8	475	0.928	0.929
LDPE/PE-g-MA/MMT-ODA 82:12:6	101.8	9.1	12.7	630	0.939	0.937

of weight loss rate for compatibilized nanocomposites, about 30–35 °C, as compared with those for other materials tested, indicates that exfoliated clay inhibits polymer decomposition in air, most probably due to improved barrier for diffusion of atmospheric oxygen into the material.

The results of the mechanical tests of the materials are collected in Table 2. The curves selected for Fig. 6 demonstrate the average stress–strain behaviour of the materials. Plastic deformation with necking was observed in all materials. The yield stress was similar for LDPE and all compatibilized compositions, at about 9 MPa, and slightly larger, at about 9.5 MPa for noncompatibilized LDPE/MMT 94:6 wt.% system. Other mechanical parameters, like elongation and stress at break, depended strongly on the clay content and its dispersion. Noncompatibilized composition of LDPE with MMT-ODA exhibits poor drawability in contrast to the compatibilized nanocomposite with the same clay content of 6 wt.% The elongation achieved for the nanocomposite with 6 wt.% of MMT-ODA, larger than that for the nanocomposite with 3 wt.% of MMT-ODA, resulted from the exfoliation of clay particles and was also caused by a relatively high content of a compatibilizer. LDPE/PE-g-MA blend exhibited lower yield stress and larger elongation to break than neat LDPE. The presence of MMT-ODA clay in LDPE causes an increase, while the presence of relatively soft

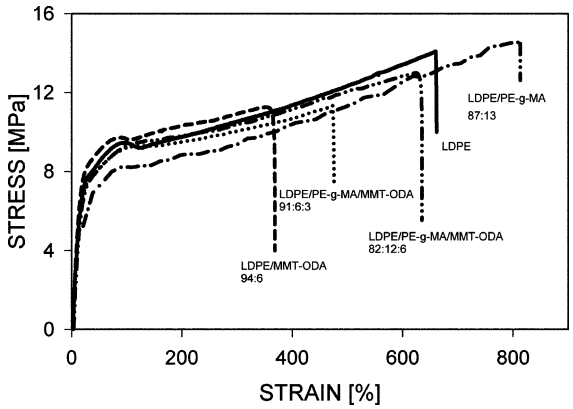

Fig. 6. Stress–strain dependencies during tensile drawing for: LDPE/PE-g-MA 97:13 wt.% LDPE, LDPE/PE-g-MA/MMT-ODA 82:12:6 wt.%, LDPE/PE-g-MA/MMT-ODA 91:6:3 wt.% and LDPE/MMT-ODA 94:6 wt.%.

compatibilizer causes a decrease of the modulus of elasticity. The modulus of compatibilized systems was lower than that of neat LDPE and its value increased slightly with the nanofiller content. The highest modulus increase, by 10%, was observed in the noncompatibilized system.

As it follows from Table 2 the density of samples after deformation increased slightly except for the sys-

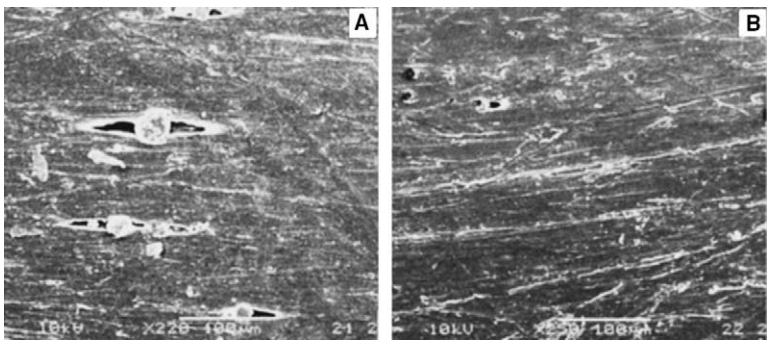

Fig. 7. SEM micrographs of surfaces of deformed samples of LDPE/MMT-ODA 94:6 wt.% (A) and LDPE/PE-g-MA/MMT-ODA 82:12:6 wt.% (B).

tem LDPE/MMT-ODA 94:6 wt.%, where it decreased by approximately 5%. The SEM studies of surfaces of deformed samples revealed a significant amount of cavities around clay inclusions in the noncompatibilized system, while only occasional, and much smaller cavities were found in the compatibilized nanocomposites (Fig. 7). Those results demonstrate that in the noncompatibilized system a decohesion of the matrix from clay particles occurs during deformation, which causes the premature breakup of samples.

4. Conclusions

A nanocomposite of LDPE with MMT-ODA having tensile properties comparable with pure LDPE can be obtained by melt mixing along the route consisting of a masterbatch preparation of a compatibilizer with filler using as a compatibilizer-maleic anhydride grafted ultra low density polyethylene. The exfoliation of clay platelets leads to an improved thermal stability of the composite in air. The noncompatibilized composite of LDPE and MMT-ODA fractures early during drawing due to decohesion of the polymer from nonexfoliated clay particles and does not exhibit improved thermal stability. However, the mechanical performance of the system is not governed only by the clay exfoliation and clay content but also by the presence of a significant amount of the compatibilizer. The compatibilized nanocomposite LDPE/PE-g-MA/MMT-ODA 82:12:6 wt.% contains more nonexfoliated clay tactoids than LDPE/PE-g-MA/MMT-ODA 91:6:3 wt.%, as it follows from WAXS studies, however, it can be deformed to higher elongation. Thus, maleic anhydride grafted polyethylene not only promotes the exfoliation of the clay and its good adhesion to LDPE but it also toughens the polymer matrix.

Acknowledgment

This work was partially supported by the State Committee for Scientific Research (Poland) through Technical University of Lodz and Centre of Molecular and Macromolecular Studies, PAS, under Grant PBZ 13/T08/99.

References

[1] Gorrasi G, Tortora M, Vittoria V, Pollet E, Lepoittevin B, Alexandre M, et al. Vapor barrier properties of polycaprolactone montmorillonite nanocomposites: effect of clay dispersion. Polymer 2003;44:2271–9.

[2] Wang SF, Hu Y, Li ZL, Zhuang YL, Chen Zy, Fan WC. Flammability and phase-transition studies of nylon 6/montmorillonite nanocomposites. Colloid Polym Sci 2003;281:951–6.

[3] Hasegawa N, Okamoto H, Kato M, Usuki A, Sato N. Nylon 6/Na-montmorillonite nanocomposites prepared by compounding nylon 6 with Na-montmorillonite slurry. Polymer 2003;44:2933–7.

[4] Biswas M, Ray SS. Recent progress in synthesis and evaluation of polymer–montmorillonite nanocomposites. Adv Polym Sci 2001;155:167–221.

[5] Maiti P, Nam PH, Okamoto M, Hasegawa N, Usuki A. Influence of crystallization on intercalation, morphology, and mechanical properties of polypropylene/clay nanocomposites. Macromolecules 2002;35:2042–9.

[6] Svoboda P, Zeng Ch, Wang H, Lee J, Tomasko DL. Morphology and mechanical properties of polypropylene/organoclay nanocomposites. J Appl Polym Sci 2002;85:1562–70.

[7] Manias E, Touny A, Wu L, Strawhecker K, Lu B, Chung TC. Polypropylene/montmorillonite nanocomposites. Review of the synthetic routes and materials properties. Chem Mater 2001;13:3516–23.

[8] Hasegawa N, Okamoto H, Kato M, Tsukigase A, Usuki A. Polyolefin–clay hybrids based on modified polyolefins and organophilic clay. Macromol Mater Eng 2000;280:76–9.

[9] Kawasumi M, Hasegawa N, Kato M, Usuki A, Okada A. Preparation and mechanical properties of polypropylene–clay hybrids. Macromolecules 1997;30:6333–8.

[10] Heinemann J, Reichert P, Thomann R, Mulhaupt R. Polyolefin nanocomposites formed by melt compounding and transition metal catalyzed ethene homo- and copolymerization in the presence of layered silicates. Macromol Rapid Commun 1999;20:423–30.

[11] Jin YH, Park HJ, Im SS, Kwak SY, Kwak S. Polyethylene/clay nanocomposite by in-situ exfoliation of montmorillonite during Ziegler–Natta polymerization of ethylene. Macromol Rapid Commun 2002;23:135–40.

[12] Alexandre M, Dubois P, Sun T, Garces JM, Jerome R. Polyethylene-layered silicate nanocomposites prepared by the polymerization-filling technique: synthesis and mechanical properties. Polymer 2002;43:2123–32.

[13] Gopakumar TG, Lee JA, Kontopoulou M, Parent JS. Influence of clay exfoliation on the physical properties of montmorillonite/polyethylene composites. Polymer 2002;43:5483–91.

[14] Koo CM, Ham HT, Kim SO, Wang KH, Chung IJ, Kim DC, et al. Morphology evolution and anisotropic phase formation of the maleated polyethylene-layered silicate nanocomposites. Macromolecules 2002;35:5116–22.

[15] Wang KH, Choi MH, Koo ChM, Choi YS, Chung IJ. Synthesis and characterization of maleated polyethylene/clay nanocomposites. Polymer 2001;42:9819–26.

[16] Wang KH, Choi MH, Koo CM, Xu MZ, Chung IJ, Jang MC, et al. Morphology and physical properties of polyethylene/silicate nanocomposite prepared by melt intercalation. J Polym Sci, Part B: Polym Phys 2002;40:1454–63.

[17] Kato M, Okamoto H, Hasegawa N, Tsukigase A, Usuki A. Preparation and properties of polyethylene–clay hybrids. Polym Eng Sci 2003;43:1312–6.

[18] Liang G, Xu J, Bao S, Xu W. Polyethylene/maleic anhydride grafted polyethylene/organic montmorillonite

nanocomposites. I. Preparation, microstructure, and mechanical properties. J Appl Polym Sci 2004;91: 3974–80.

[19] Morawiec J, Pawlak A, Slouf M, Galeski A, Piorkowska E. Influence of compatibilizer type, polypropylene molecular weight and blending sequence on montmorillonite exfoliation in nanocomposites. Polimery 2004;49:51–4.

[20] Xu W, Ge M, He P. Nonisothermal crystallization kinetics of polypropylene/montmorillonite nanocomposites. J Polym Sci, Part B: Polym Phys 2002;40:408–14.

[21] Pozsgay A, Frater T, Papp L, Sajo I, Pukanszky B. Nucleating effect of montmorillonite nanoparticles in polypropylene. J Macromol Sci Part B: Phys 2002;41: 1249–65.

[22] Nowacki R, Monasse B, Piorkowska E, Galeski A, Haudin JM. Spherulite nucleation in isotactic polypropylene based nanocomposites with montmorilonite under shear. Polymer 2004;45:4877–92.

[23] Wunderlich B, Czornyj G. A study of equilibrium melting of polyethylene. Macromolecules 1977;10:906–13.